

Generation of lattices of optical vortices

A. Dreischuh*, S. Chervenkov, D. Neshev¹, G. G. Paulus², and H. Walther^{2,3}

Department of Quantum Electronics, Sofia University, 5 James Bourchier Blvd.,
BG-1164 Sofia, Bulgaria

¹Laser Centre, Vrije Universiteit Amsterdam, De Boelelaan 1081, 1081 HV Amsterdam,
The Netherlands

²Max-Planck-Institut für Quantenoptik, Hans-Kopfermann-Str. 1, D-85748 Garching, Germany

³Sektion Physik, Ludwig-Maximilians-Universität München, Am Coulombwall 1,
D-85748 Garching, Germany

ABSTRACT

Square and hexagonal lattices of optical vortices are generated in a saturable nonlinear medium. If the topological charges of the vortices are of the same sign the lattice exhibit rotation, while if alternative, stable propagation of the structures is observed. In a nonlinear medium vortex lattices induce periodic modulation of the refractive index. Diffraction of a probe beam by this optically-induced phase grating is observed.

Keywords: Optical vortex, topological charge, vortex lattice, nonlinearity, diffraction

1. INTRODUCTION

Optical vortices are intriguing objects that attract much attention¹ and display fascinating properties with possible applications in the optical transmission of information and in guiding and trapping of particles. Vortices can be generated in several different controllable ways in lasers with large Fresnel numbers², by helical phase plates³, laser mode converters⁴, or computer-generated holograms (CGHs)⁵. The last method, however, is the most commonly used, since it allows precise control of the vortex position, topological charge (TC), and possibility for generation of specific patterns of optical vortices. Optical vortex solitons (OVs) are first experimentally generated in Kerr nonlinear medium (NLM)⁶ and later in media with other types of nonlinearity: saturable atomic⁷, photorefractive⁸, and photovoltaic⁹. The propagation of multiply charged OVs¹⁰ is found to be unstable and the dark beams decay into vortices of unit charge¹¹. While interacting with each other by phase and intensity gradients the vortices can arrange themselves in regular patterns (vortex lattices). The simplest case of square lattice consisting of vortices with alternative charges was investigated by direct modeling of four of them under periodic boundary conditions¹². Later, lattices with different geometries imposed on a finite background beam (conditions closer to the experimental ones) were considered¹³. It was shown that depending on the TCs the vortex lattices can exhibit rotation or rigid propagation for equal or alternative TCs, respectively. In addition, lattices possess elasticity against displacement of one or more vortices out of their equilibrium positions.

Here we report numerical and experimental investigation of lattice structures of optical vortices in self-defocusing NLM. We concentrate our attention on two types of lattice geometries - square and hexagonal one. When propagating in the NLM they induce a periodic modulation of its refractive index. For high beam intensities these changes are sufficient to cause a diffraction of a probe beam propagating perpendicularly to the volume with periodically modulated refractive index.

2. COMPARATIVE NUMERICAL AND EXPERIMENTAL RESULTS

The evolution of the structured beams in a self-defocusing NLM with saturable nonlinearity is described by the normalized Schrödinger equation for the slowly varying amplitude envelope

$$i\partial E/\partial z + (1/2)\Delta_{\perp}E - |E|^2E/(1+s|E|^2) = 0 \quad , \quad (1)$$

* E-mail:ald@phys.uni-sofia.bg

where Δ_{\perp} is the transverse Laplace operator. The transverse coordinates (x,y) are normalized to the optical vortex radius a , and the propagation coordinate z is normalized to the diffraction length of the dark beams. The background beam intensity $I=|E|^2$ is expressed in units of the intensity I_{1Dsol} necessary for forming an one-dimensional dark spatial soliton of a width equal to the OV radius a . The saturation parameter is defined by $s=I_{1Dsol}/I_{sat}$, where I_{sat} is the saturation intensity retrieved from the experimental conditions. The model of the saturation is introduced phenomenologically. In all measurements reported here we used thermal NLM – ethylene glycol dyed with DODCI (diethyloxadycarbocyanine iodine). For the two concentrations of the dye used the parameters of the nonlinear response function were $s=0.2, 1.2$; $\gamma=3$ in both cases.

To investigate the propagation dynamics of vortex lattices we conducted numerical simulations by using the beam propagation method. The initial conditions were modeled as superposition of vortices situated in the nodes of lattices

$$E(r, z = 0) = \prod_{j,k=-\infty}^{\infty} \begin{cases} sq(r - r_{jk}) \\ hex(r - r_{jk}) \end{cases}, \quad (2)$$

with square (*sq*) and hexagonal (*hex*) symmetry. In the above equation r_{ij} are the nodes of the Bravais lattice that represents the physical lattice structure, and Δ is used to denote the distance (in units of OV radius a) between two neighboring vortices. The lattice structures are modeled as superimposed upon super-Gaussian (flat-topped) background beams of widths $\omega > 40a$. Simulated grayscale images of lattices of different geometries and different TC distributions are shown in Fig. 1.

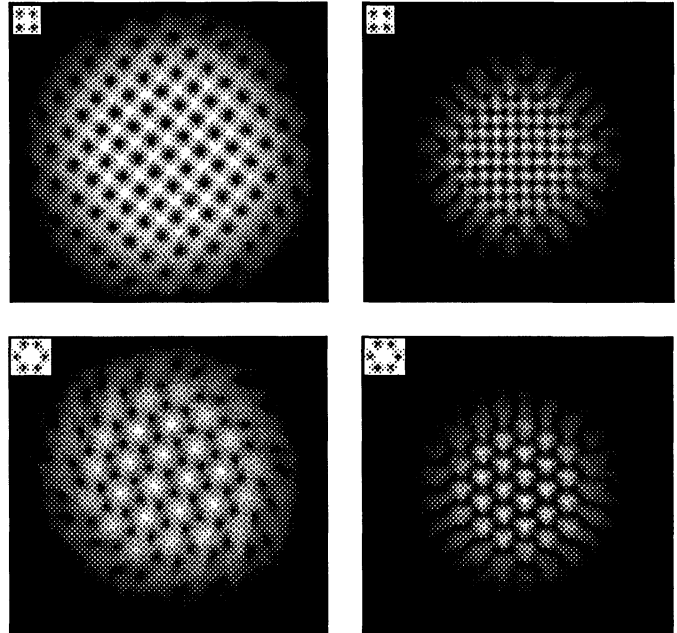


Figure 1: Background beams carrying vortex lattices with equal (left column) and alternating TCs (right column) after passing 10 nonlinear lengths along the NLM. First row – square-shaped lattices, second row – hexagonal lattices. Insets – initial elementary cells of the lattices. All other parameters for the simulations are the same ($\Delta=5.0$, $l_0=1$, and $s=0.4$).

There are no qualitative differences in the propagation of the structures with respect to the lattice geometry (square or hexagonal). The propagation, however, depend crucially on the vortex charge distribution (equal, left column, or alternating, right column). Two characteristic differences are clearly seen in Fig. 1: (i) In the case of equal TCs the superposition of the phases of all vortices results in an azimuthal phase gradient and a non-zero angular momentum, which causes rotation of the whole structure. In the case of alternating TCs the superposition gives, on average, zero total angular momentum. As a result, steady propagation of the lattices with alternating TCs is observed in the simulations (Fig. 1, right column). (ii) In the case of equal TCs the nonzero angular momentum and the vortex repulsion lead to increased broadening of the background beam along the NLM. The dependence of the beam propagation on the intensity in this case is relatively weak, since the topological effects dominate the nonlinear ones.

The experimental setup is shown in Fig. 2. The 488-nm line from an Ar^+ laser is used to reconstruct photolithographically produced CGHs of the respective vortex lattices. The +1 (or -1) order of the diffraction was separated from the other diffraction orders by an iris diaphragm and was focused near the input face of a glass cell containing the NLM. The output face of the cell was imaged to a CCD camera, and neutral filters were used to prevent its saturation.

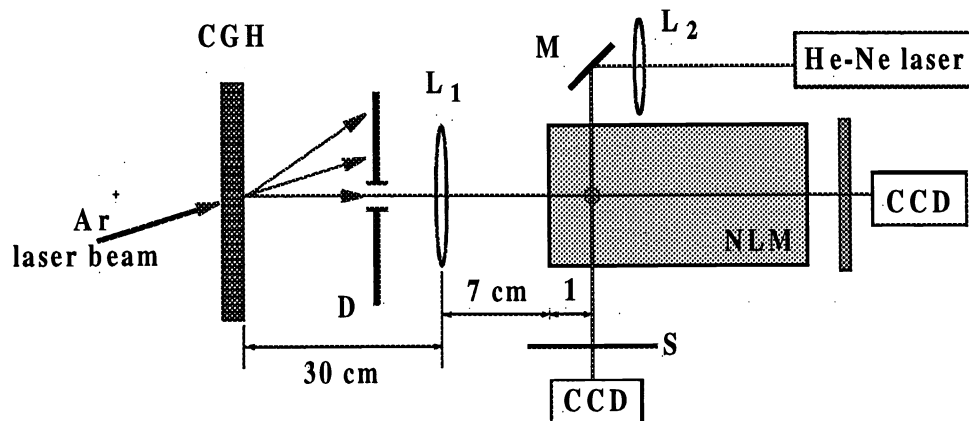


Figure 2: Experimental setup: D, diaphragm; L_1 , L_2 , lenses of focal lengths 7.0 and 8.0 cm, respectively; M – mirror; S, screen; CCD, charge-coupled device camera. The characteristic distances between elements are shown.

The correct reproduction of the CGHs was verified by the characteristic interference patterns when the diaphragm is open and the +1 diffraction order do interfere with the 0th order. Because of some technical restrictions in synthesizing the gratings, for the lattice with equal TCs the number of vortices encoded is less than in the hologram with alternating TCs.

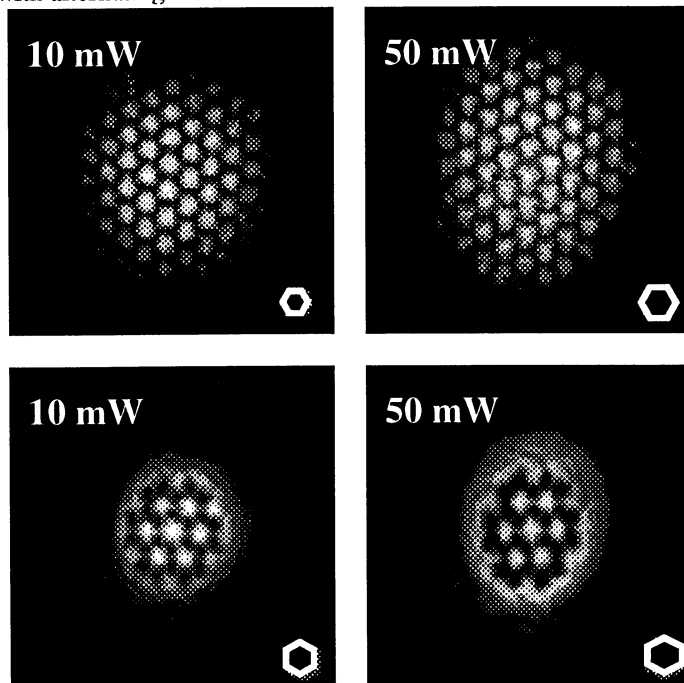


Figure 3: Images of the vortex lattices recorded after 10-cm propagation in a NLM.

First row – hexagonal lattice with alternating TCs for powers of 10 and 50 mW.
 Second row – hexagonal lattice with equal TCs for the same powers.
 The insets represent the size and orientation of the elementary cell of each lattice.

As seen in Fig. 3, the propagation behavior of the lattices is clearly different depending on the TC distribution. Whereas the lattice with alternating TCs exhibits steady propagation (Fig. 3, upper row), the lattice with equal charges tends to rotate. The background beam spread more widely than in the case of a lattice with alternating charges. Because the distances between the neighboring vortices were encoded in the CGHs to be the same, any difference in vortex separation is due to evolution during propagation. The insets in Fig. 3 are intended to visualize the exact size and orientation of the elementary cell of the lattice. The comparison for the two cases shows that the one with equal TCs is 18% larger. The influence of the nonlinearity can be seen if the corresponding images for two powers are compared. For 50 mW power we estimated 15% and 12% broadening for alternating and equal TCs, respectively. That difference we attributed to the topological interaction of equally charged vortices between the CGH and the NLM. Square-shaped lattices were investigated in the same way, and qualitatively similar features were observed.

3. DIFFRACTION OF A PROBE BEAM BY VORTEX LATTICE

When an intense laser beam propagates along a NLM, its refractive index changes proportionally to the intensity distribution. Inasmuch as the vortex lattices possess a periodic intensity distribution one can expect periodic modulation of the refractive index. In a self-defocusing medium the higher local intensity corresponds to a lower local refractive index. The lattices are imposed on a finite background beam, which induces in the NLM a cylindrical defocusing lens for perpendicular propagating probe beam. This effective lens is modulated by the dark-vortex structure. In our experiment the probe beam of a single-mode He-Ne laser was aligned to cross the pump beam 1 cm inside the NLM. The input profile is shown in Fig. 4a and its circular symmetry is evident. When it crosses the Ar⁺ laser beam with no vortices nested in, the influence of optically-induced cylindrical lens are identified. The three probe beam profiles in Fig. 4b correspond to three different positions achieved by parallel vertical translation of the He-Ne laser beam. The probe beam is elongated symmetrically if it crosses the pump in the center and becomes asymmetrical if it is shifted.

The situation is different when vortex lattices are imposed on the background beam. Because of the nonlinear change in the refractive index, the vortex lattice writes a phase grating in the NLM. The perpendicularly propagating He-Ne laser passes through this grating and develops well-pronounced diffraction orders at the output screen, as shown in Fig. 4c,d. The constant of the phase grating written is apparently different for the square-shaped (Fig. 4c) and hexagonal-shaped (Fig. 4d) lattice. In the first case the period of the vortex structure was smaller (so was the period of the phase grating) and higher dispersion in the diffraction orders was observed. Because of the finite number of vortices in the lattices and the nearly equal sizes of the background and the probe beams, the diffraction from the phase grating can not be compared directly with diffraction from an infinite periodic structure. In our view the ratio between the intensities of the different diffraction orders is gradually influenced by the fact that different parts of the probe beam

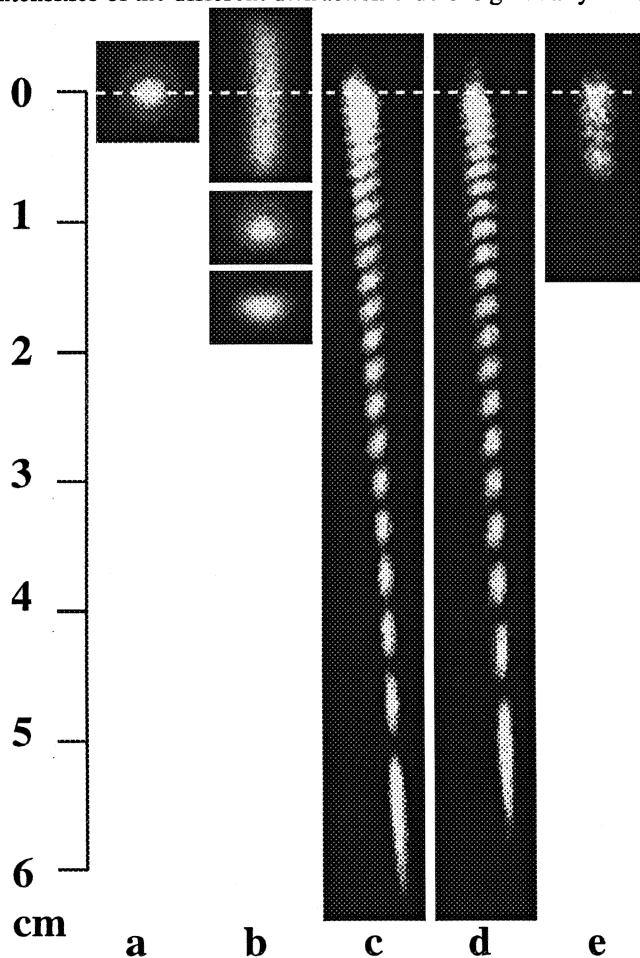


Figure 4: Images of the probe He-Ne laser beam on screen S (see Fig. 2).

- (a) Input He-Ne laser beam profile;
- (b) Profiles of the probe beam at low pump power (10 mW) for different vertical displacements with respect to the pump beam;
- (c), (d) Diffraction of the probe beam from the periodic phase gratings induced in the NLM by square and hexagonal vortex lattices, respectively. Pump power – 80 mW.
- (e) Diffraction pattern when a single vortex is superimposed upon the pump beam. Pump power 30 mW.

pass through different number of vortices. Further, at the exit of the phase grating the modulated probe beam is affected additionally by the aberrations of the thermal lens. As shown in Fig. 4e, diffraction by a single vortex is substantially different. In all experiments we observed strong vertical asymmetry of the probe-beam diffraction pattern, which developed at powers higher than 20 mW.

4. CONCLUSION

We successfully experimentally generated lattice structures of optical vortices with different topological charge distributions in saturable nonlinear media. Because of the intensity dependence of the refractive index these lattices induce periodic modulation of the refractive index of the medium and write effective phase gratings in it. The modulation is sufficient to force perpendicularly propagating probe laser beam to diffract¹⁴. This property could offer the interesting possibility of creating periodic structures in the refractive index of NLM for optical writing of two-dimensional photonic crystals.

ACKNOWLEDGMENTS

A. Dreischuh thanks the Alexander-von-Humboldt foundation for a fellowship and for facilitating the measurements that he made at the Max-Planck-Institut für Quantenoptik (Garching, Germany). The research of D. Neshev was partially supported by a Marie-Curie fellowship under contract HPMFCT-2000-00455. The authors thank Yu. Kivshar, L. Torner, A. Desyatnikov, and N. Herschbach for valuable discussions and support of this research.

References:

1. M. Vasnnetsov, K. Staliunas, eds., *Optical Vortices* (Nova Science, New York, 1999).
2. P. Coullet, L. Gil, F. Rocca, "Optical vortices," *Opt. Commun.* **73**, pp. 403-408, 1989.
3. M.W. Beijersbergen, R.P.C. Coerwinkel, M. Kristiasen, and J.P. Woerdman, "Helical wave-front laser beams produced with a spiral phaseplate," *Opt. Commun.* **112**, pp. 321-327, 1994.
4. Chr. Tamm and C.O. Weiss, "Bistability and optical switching of spatial patterns in a laser," *J. Opt. Soc. Am.* **B7**, pp. 1034-1038, 1990; D.V. Petrov, F. Canal, and L. Torner, "A simple method to generate optical beams with a screw phase dislocation," *Opt. Commun.* **143**, pp. 265-267, 1997.
5. N.R. Heckenberg, R. McDuff, C.P. Smith, and A.G. White, "Generation of optical phase singularities by computer-generated holograms," *Opt. Lett.* **17**, pp. 221-223, 1992.
6. G.A Swartzlander, Jr. and C.T Law, "Optical vortex solitons observed in Kerr nonlinear media," *Phys. Rev. Lett.* **69**, pp. 2503-2506, 1992.
7. V. Tikhonenko, Yu.S. Kivshar, V.V. Steblina, A.A. Zozulya, "Vortex solitons in a saturable optical medium," *J. Opt. Soc. Am.* **B15**, pp. 79-86, 1998.
8. G. Duree, M. Morin, G. Salamo, M. Segev, B. Crosignani, P. Di Porto, E. Sharp, and A. Yariv, "Dark photorefractive spatial solitons and photorefractive vortex solitons," *Phys. Rev. Lett.* **74**, pp. 1978-1981, 1995.
9. Z. Chen and M. Segev, "Self-trapping of an optical vortex by use of the bulk photovoltaic effect," *Phys. Rev. Lett.* **78**, pp. 2948-2951, 1997.
10. A.V. Mamaev, M. Saffman, and A.A. Zozulya, "Decay of high order optical vortices in anisotropic nonlinear optical media," *Phys. Rev. Lett.* **78**, pp. 2108-2111, 1997; I. Velchev, A. Dreischuh, D. Neshev, and S. Dinev, "Multiple-charged optical vortex solitons in bulk Kerr media," *Opt. Commun.* **140**, pp. 77-82, 1997.
11. A. Dreischuh, G.G. Paulus, F. Zacher, F. Grabson, D. Neshev, and H. Walther, "Modulational instability of multiple-charged optical vortex solitons under saturation of the nonlinearity," *Phys. Rev.* **E60**, pp. 7518-7524, 1999.
12. G.S. McDonald, K.S. Sayed, and W.J. Firth, "Optical vortices in beam propagation through a self-defocusing medium," *Opt. Commun.* **94**, pp. 469-476, 1992.
13. D. Neshev, A. Dreischuh, M. Assa, and S. Dinev, "Motion control of ensembles of ordered optical vortices generated on finite extent background," *Opt. Commun.* **151**, pp. 413-421, 1998.
14. A. Dreischuh, S. Chervenkov, D. Neshev, G. G. Paulus, and H. Walther, "Generation of lattice structures of optical vortices," *J. Opt. Soc. Am. B* **19**, pp. 550-556, 2002.